NUKLEONIKA 2017;62(2):117–122
doi: 10.1515/nuka-2017-0016

ORIGINAL PAPER

Compositional dependence of hyperfine interactions and magnetoelectric coupling in $(BiFeO_3)_x$-$(BaTiO_3)_{1-x}$ solid solutions

Karol Kowal, Piotr Guzdek, Maciej Kowalczyk, Elżbieta Jartych

Abstract. In this work the compositional dependence of hyperfine interactions and magnetoelectric coupling in $(BiFeO_3)_x$-$(BaTiO_3)_{1-x}$ solid solutions where $x = 0.5$–0.9 fabricated from commercial $BaTiO_3$ in terms of the solid-state sintering method at various temperatures and over different time periods is described. In general, as the content of $BaTiO_3$ increases, a decrease in the hyperfine magnetic field (B_{hf}) at ^{57}Fe nuclei was observed. However, for samples exhibiting lower homogeneity in which the ions of Bi^{3+} and Fe^{3+} are replaced by Ba^{2+} and Ti^{4+} with lower probability, higher values of B_{hf} are obtained. For the sample where $x = 0.6$ that exhibits the coexistence of rhombohedral, regular and tetragonal phases, the highest value of the α_{ME} coefficient (3.57 mV/A) was observed, which is more than three times higher when compared to the hitherto published results.

Keywords: hyperfine interactions • magnetoelectric coupling • Mössbauer spectroscopy

K. Kowal✉, E. Jartych
Institute of Electronics and Information Technology,
Lublin University of Technology,
38A Nadbystrzycka Str., 20-618 Lublin, Poland,
Tel.: +48 81 538 4464, Fax: +48 81 538 4312,
E-mail: k.kowal@pollub.pl

P. Guzdek
Institute of Electron Technology, Cracow Division,
39 Zabłocie Str., 30-701 Kraków, Poland

M. Kowalczyk
Faculty of Materials Science and Engineering,
Warsaw University of Technology,
141 Wołoska Str., 02-507 Warsaw, Poland

Received: 31 July 2016
Accepted: 8 October 2016

Introduction

The promise of coupling between magnetization and electric polarization and the potential to manipulate one through the other has become in recent years a driving force for many experimental works on multiferroic materials. The ultimate goal of these studies would be a single-phase material exhibiting a strong coupling between inherent ferromagnetic and ferroelectric ordering at room temperature. Magnetoelectric coupling is characterized by the magnetoelectric voltage coefficient α_{ME} which describes the change in the magnetically induced electric field per unit of the applied magnetic field [1].

Recently, magnetoelectric coupling at room temperature was found to exhibit significant magnitudes in the single-phase electroceramics of $(BiFeO_3)_x$-$(BaTiO_3)_{1-x}$ synthesized by the solid-state sintering method [2]. By appropriately refining the chemical composition of these materials and their processes of synthesis, our group has even achieved up to 66% higher values of the α_{ME} coefficient [3]. Driven by the desire to understand the mechanism of the magnetoelectric effect which occurs in these materials, additional experiments involving X-ray diffraction (XRD), ^{57}Fe Mössbauer spectroscopy (MS), and vibrating sample magnetometry (VSM) were conducted. The measurements were made for two series of samples fabricated from: (1) precursor oxides Bi_2O_3, Fe_2O_3, TiO_2, and barium carbonate ($BaCO_3$) [4]; and (2) commercial barium titanate ($BaTiO_3$) (instead of TiO_2 and $BaCO_3$) [3]. The

gradual structural transformation from rhombohedral to regular was supposed for both series of samples with x decreasing from 0.9 to 0.7 based on the qualitative phase analysis of the obtained X-ray diffraction patterns.

The aim of this work was a thorough study of how hyperfine interactions and magnetoelectric coupling in $(BiFeO_3)_x$-$(BaTiO_3)_{1-x}$ solid solutions depend on their chemical compositions and fabrication processes.

Experimental details

Three variants of the solid-state sintering method differing in terms of the sintering temperature (T = 1053, 1103, and 1153 K) and time (t = 40, 20, and 4 h, respectively) were used to prepare a series of $(BiFeO_3)_x$-$(BaTiO_3)_{1-x}$ solid solutions where x = 0.5–0.9. The samples were synthesized from precursor oxides Bi_2O_3, Fe_2O_3, TiO_2 and commercial barium titanate according to the procedure described in [5]. Before sintering, the samples where x = 0.7–0.9 were mechanically processed twice (milled and pressed under 30 MPa), while the samples where x = 0.5 and 0.6 were mechanically treated only once. This modification was introduced in order to verify how the properties of the materials are affected by their homogeneity.

Magnetic measurements were performed for all the samples to verify if they indeed possess ferromagnetic ordering, as was previously reported [6–8], and how the magnetic order parameters depend on their chemical composition. The measurements were carried out at room temperature by a vibrating sample magnetometer produced by Lake Shore Cryotronics Inc. (model 7440). A magnetic field was generated by a current in the electromagnetic coils and its value varied from –1600 to 1600 kA/m.

In order to examine the structure of the samples room temperature X-ray diffraction measurements were carried out by a Philips PW3710 diffractometer using CoK_α radiation, operating in the Bragg-Brentano geometry within the range of 2θ from 10° to 90° with a step equal to 0.008°. Structural analysis was performed using the Rietveld method implemented in the PANalytical X'Pert HighScore Plus software package.

The hyperfine interactions of $(BiFeO_3)_x$-$(BaTiO_3)_{1-x}$ solid solutions were investigated by Mössbauer spectroscopy. The Mössbauer spectra were collected at room temperature in transmission geometry using a source of ^{57}Co in a chromium matrix. The spectrometer was calibrated using a 25 μm-thick metallic iron foil.

Measurements of the magnetoelectric voltage coefficient α_{ME} were performed by a dynamic lock-in amplifier described in detail in [1]. The samples were placed in a time-varying DC magnetic field on which a small sinusoidal AC magnetic field with a frequency f_{AC} of 1 kHz was superimposed. The voltage signal induced due to the magnetoelectric

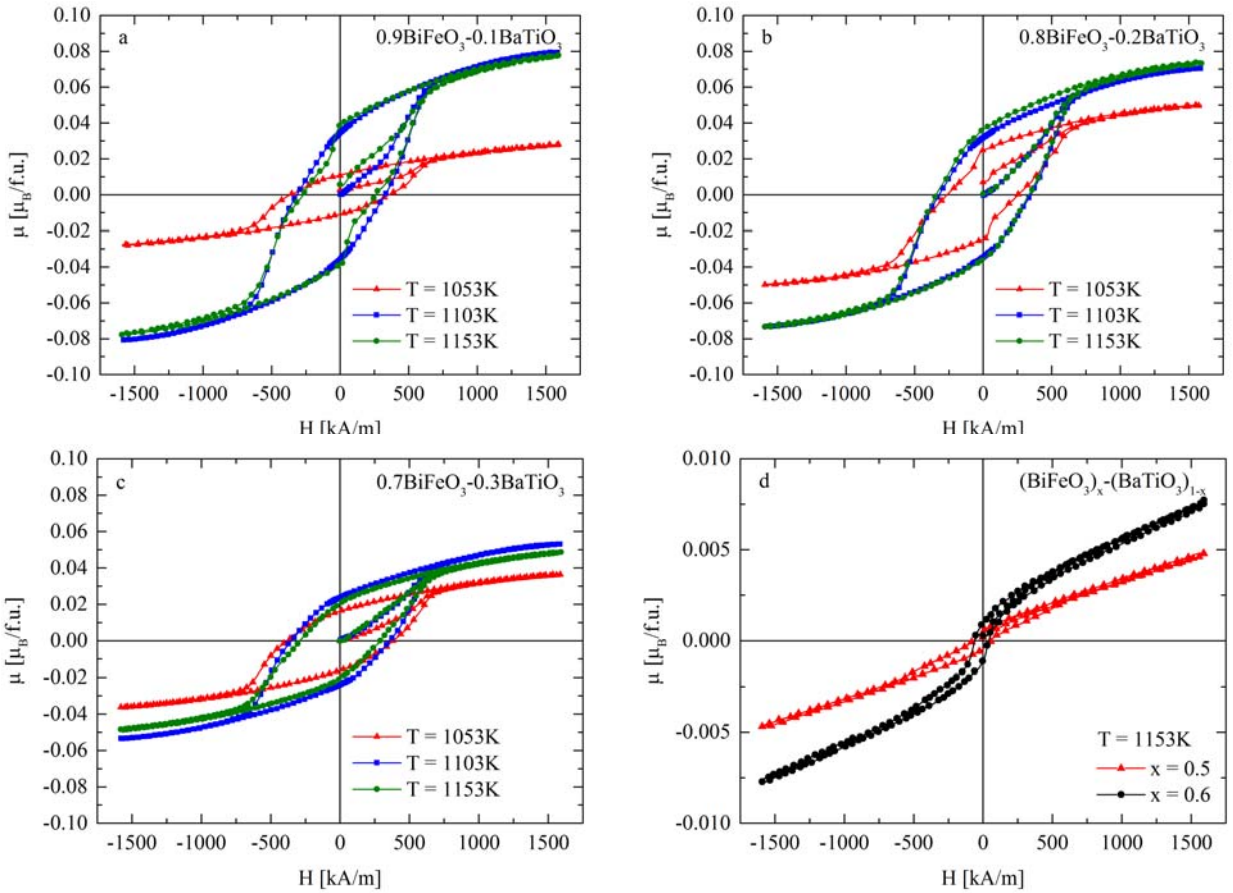

Fig. 1. Room-temperature magnetic hysteresis loops of $(BiFeO_3)_x$-$(BaTiO_3)_{1-x}$ solid solutions sintered at various temperatures: (a) x = 0.9, (b) x = 0.8, (c) x = 0.7, (d) x = 0.6 and 0.5.

Table 1. The parameters of magnetic hysteresis loops for $(BiFeO_3)_x$-$(BaTiO_3)_{1-x}$ samples with different composition sintered at various temperatures; μ_S – magnetic saturation moment, μ_R – remanence moment; μ_B – Bohr magneton, f.u. – formula unit, H_C – coercive field

Sintering method	x	μ_S [μ_B/f.u.]	μ_R [μ_B/f.u.]	H_C [kA/m]
T = 1053 K, t = 40 h	0.9	0.028	0.011	388.7
	0.8	0.050	0.025	256.5
	0.7	0.036	0.017	382.2
T = 1103 K, t = 20 h	0.9	0.079	0.037	334.8
	0.8	0.073	0.032	332.3
	0.7	0.053	0.024	336.7
T = 1153 K, t = 4 h	0.9	0.078	0.039	273.6
	0.8	0.074	0.034	350.0
	0.7	0.049	0.022	290.5
	0.6	–	0.001	64.9
	0.5	–	<0.001	82.5

effect was measured by the dynamic lock-in amplifier (Stanford Research Systems, model SR830).

Results and discussion

Although pure $BiFeO_3$ at room temperature exhibits antiferromagnetic ordering, the investigated solid solutions were found to exhibit weak ferromagnetism (Fig. 1), as has been previously reported [6–8]. The parameters of the observed hysteresis loops depend on both the chemical compositions of the samples and their sintering temperatures (Table 1). The highest values of the magnetic saturation moment μ_S were recorded for samples where x = 0.9 sintered at T = 1103 and 1153 K. This confirms that even a small amount of $BaTiO_3$ can destroy the spin cycloid of $BiFeO_3$ causing weak ferromagnetism of $(BiFeO_3)_x$-$(BaTiO_3)_{1-x}$. However, further increasing the $BaTiO_3$ concentration up to 30% leads to lower values of μ_S due to the lower concentration of magnetic Fe^{3+} ions in these samples.

The lowest magnetic response was registered for samples sintered at the lowest temperature (T = 1053 K) despite the fact that the sintering time was ten times longer than for samples sintered at 1153 K. For samples where x = 0.5 and 0.6 no saturation effect was observed (Fig. 1d). Moreover, significantly lower values of the coercive field were registered for these samples when compared to the materials with $x \geq 0$.

The results of X-ray diffraction showed that all samples of $0.9BiFeO_3$-$0.1BaTiO_3$ exhibit the rhombohedral ($R3c$) structure, characteristic for pure $BiFeO_3$, regardless of sintering time and temperature. The $BiFeO_3$ concentration in these samples is significantly higher than that of $BaTiO_3$, thus the Ba^{2+} and Ti^{4+} ions that are located in the structure of $BiFeO_3$ are so rare that there are no local densities that could exhibit a crystal structure other than $R3c$. The Rietveld refinement showed, however, the presence of the impurity $Bi_2Fe_4O_9$ (2–9% of weight) in all samples of $0.9BiFeO_3$-$0.1BaTiO_3$.

As x decreased from 0.9 to 0.7 a gradual structural transformation from rhombohedral to regular symmetry was observed based on the qualitative phase analysis of the X-ray diffraction patterns (Fig. 2a). The results of Rietveld analysis confirmed this observation and showed that the samples where x = 0.7 and 0.8 are two-phase solid solutions. The rhombohedral ($R3c$) and regular ($Pm3m$) structures coexist in these materials with different weight ratios depending on both chemical composition and

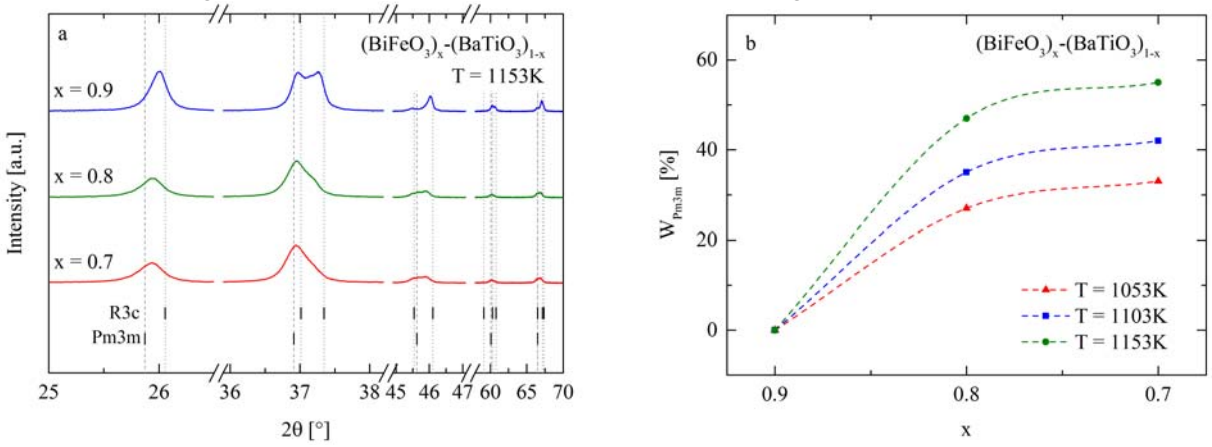

Fig. 2. (a) X-ray diffraction patterns of $(BiFeO_3)_x$-$(BaTiO_3)_{1-x}$ solid solutions where x = 0.7–0.9 sintered at T = 1153 K. (b) Mass fraction of the regular phase ($Pm3m$) determined by the Rietveld analyses for samples of various compositions x sintered at various temperatures T.

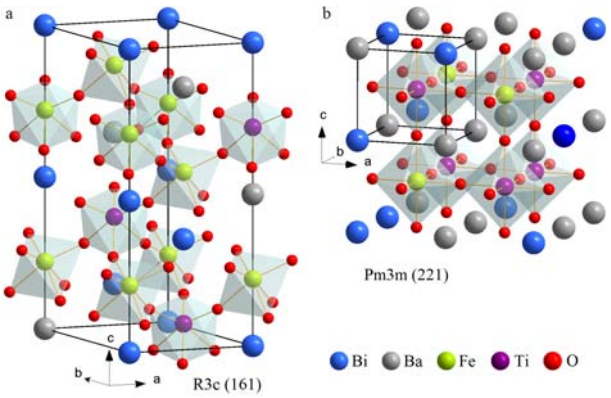

Fig. 3. Random substitution of bismuth and iron ions with barium and titanium ones and *vice versa*: (a) rhombohedral structure of $BiFeO_3$ in a hexagonal setting, (b) regular structure.

sintering parameters (Fig. 2b). The ions of bismuth and iron located in the rhombohedral structure are randomly replaced by barium and titanium ions, respectively, and *vice versa* the ions of barium and titanium located in the regular structure are randomly replaced by bismuth and iron (Fig. 3), respectively. Moreover, the volume of the rhombohedral unit cell increases as the concentration of $BaTiO_3$ increases due to the difference between the ionic radii of Bi^{3+} (103 pm) and Ba^{2+} (135 pm). The gradual structural transformation of $(BiFeO_3)_x$-$(BaTiO_3)_{1-x}$ has been described in many research papers [6–14], however, its confirmation by the Rietveld method has been demonstrated in only a couple of them [8, 11].

As the concentration of $BaTiO_3$ increases further ($x < 0.7$) one might expect the presence of an ever increasing amount of the regular phase, until the concentration of $BaTiO_3$ becomes so high (about 95% [12]) that the tetragonal structure, characteristic for pure barium titanate, forms. However, in this study the samples where $x = 0.6$ and 0.5 were prepared with limited mechanical processing. Milling and pressing were conducted only once on them, while for the other samples these processes were repeated. This limitation caused lower homogeneity of the samples where $x = 0.6$ and 0.5 when compared to the other materials. The substitution of bismuth and iron ions with barium and titanium ones was significantly reduced because of this. The reduction in the rate of substitution of these ions caused in turn the presence of a tetragonal phase in these samples. In the case of $x = 0.6$, three phases were identified (Fig. 4a), namely rhombohedral *R3c* (51%), regular *Pm3m* (42%) and tetragonal *P4mm* (7%). For $0.5BiFeO_3$-$0.5BaTiO_3$ the Rietveld analysis revealed two phases (Fig. 4b), i.e. rhombohedral (51%) and tetragonal (49%). Unfortunately, due to the intensive signal originating from the sample holder, this estimation of the relative contribution of the phases is uncertain [15].

The Mössbauer measurements showed that the hyperfine interactions depend more strongly on the composition of the samples than on the sintering time and temperature. For all samples the spectra are six-line patterns with doublet components in their central part (Fig. 5a). In the case of $x = 0.9$ the doublets are attributed to the paramagnetic $Bi_2Fe_4O_9$ phase and their parameters (isomer shift: $\delta_1 = 0.24$–0.25 mm/s, $\delta_2 = 0.35$–0.36 mm/s; and quadrupole splitting: $\Delta_1 = 0.94$–0.95 mm/s, $\Delta_2 = 0.36$–0.37 mm/s) are in good agreement with the literature [16]. For samples where $x = 0.8$ and 0.7, the doublets with parameters $\delta = 0.35$–0.37 mm/s and $\Delta = 0.51$–0.52 mm/s may be related to the regular phase present in these samples. As the content of $BaTiO_3$ increases the area of the doublets becomes larger due to the increase in the quantity of the regular phase. Simultaneously, the spectra become broadened due to the random distribution of Fe^{3+} ions substituted by Ti^{4+} within the structure of $(BiFeO_3)_x$-$(BaTiO_3)_{1-x}$ solid solutions. The best numerical fitting of the spectra was obtained by applying a probability distribution of the magnetic hyperfine field (B_{hf}) at ^{57}Fe nuclei with fixed quadrupole components (Fig. 5b). The mean value of B_{hf} determined from these distributions decreases as $BaTiO_3$ content increases from 46.4 to 46.8 T when $x = 0.9$; and 42.7 to 42.9 T when $x = 0.7$ (Fig. 5c). These values are in good agreement with previously reported results [4, 6].

The parameters of hyperfine interactions for $0.6BiFeO_3$-$0.4BaTiO_3$ and $0.5BiFeO_3$-$0.5BaTiO_3$ do not fit these trends observed for samples where

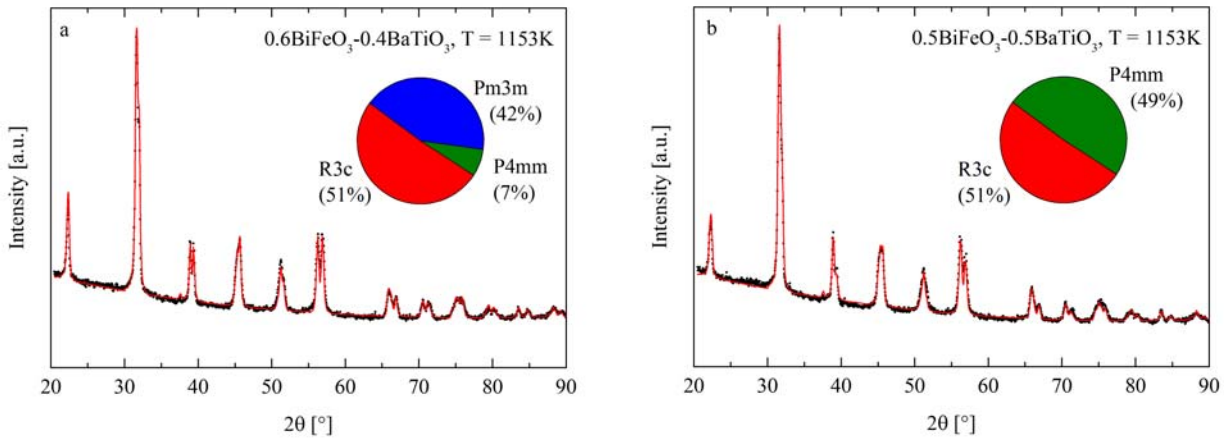

Fig. 4. X-ray diffraction patterns and results of the Rietveld analysis of: (a) $0.6BiFeO_3$-$0.4BaTiO_3$, (b) $0.5BiFeO_3$-$0.5BaTiO_3$.

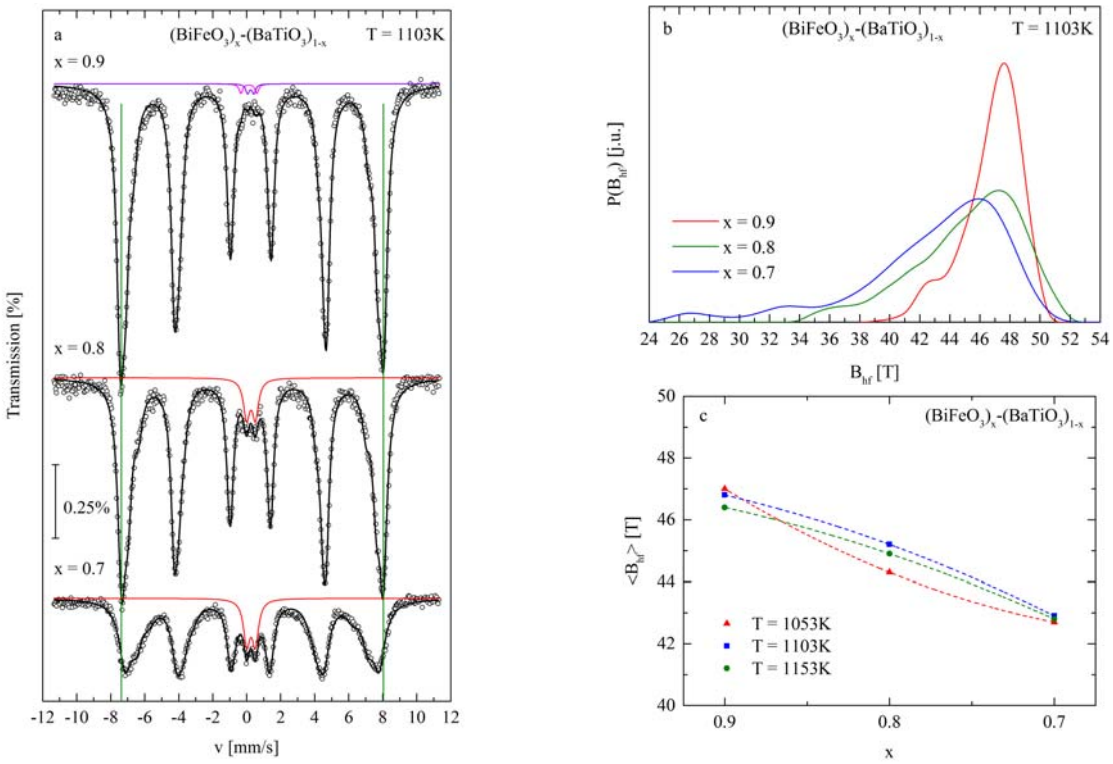

Fig. 5. (a) Room-temperature Mössbauer spectra of $(BiFeO_3)_x$-$(BaTiO_3)_{1-x}$ solid solutions sintered at T = 1103 K in terms of x. (b) Magnetic hyperfine field distributions for $(BiFeO_3)_x$-$(BaTiO_3)_{1-x}$ solid solutions sintered at T = 1103 K in terms of x. (c) Mean value of B_{hf} for samples of different chemical compositions x sintered at various temperatures T.

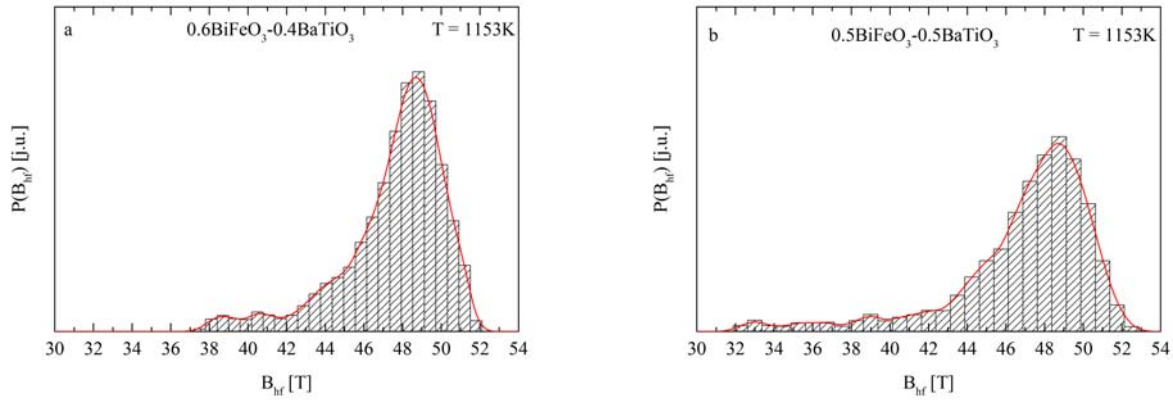

Fig. 6. Magnetic hyperfine field distributions for samples where: (a) x = 0.6, (b) x = 0.5.

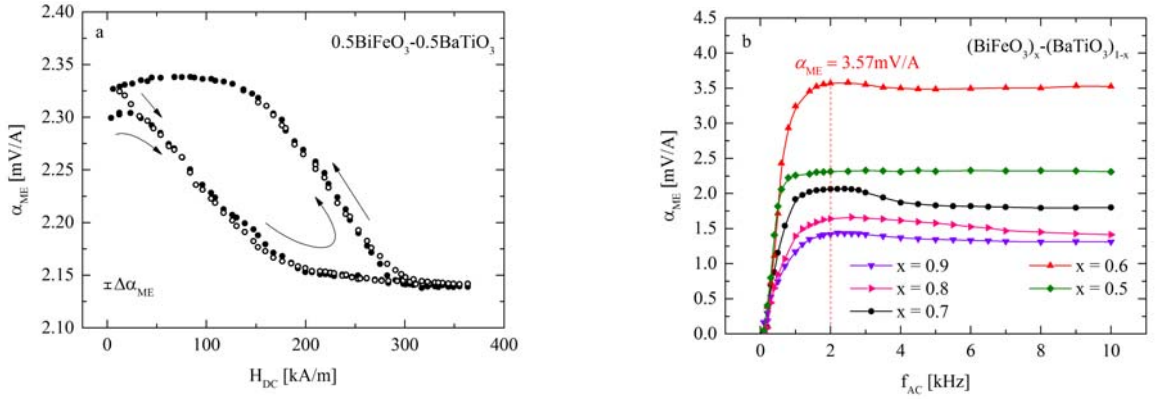

Fig. 7. (a) Variation of the magnetoelectric voltage coefficient α_{ME} in terms of the DC magnetic field for the sample where x = 0.5. (b) The frequency dependence of α_{ME} for $(BiFeO_3)_x$-$(BaTiO_3)_{1-x}$ solid solutions of various chemical compositions (x = 0.5–0.9) sintered at T = 1153 K.

x = 0.9–0.7. In particular, the probability distributions of the magnetic hyperfine field are significantly narrower and thus the mean value of B_{hf} is relatively high, i.e. 47.7 T when x = 0.6 and 47.1 T when x = 0.5 (Fig. 6). This effect is caused by the inhomogeneity of these samples.

However, it may be supposed that the inhomogeneity leading to the occurrence of the tetragonal phase in $0.5BiFeO_3$-$0.5BaTiO_3$ and multiphase structure of $0.6BiFeO_3$-$0.4BaTiO_3$ promotes stronger magnetoelectric coupling. As seen in Fig. 7a, the maximum α_{ME} value measured for $0.5BiFeO_3$--$0.5BaTiO_3$ is equal to 2.34 mV/A which is more than twice the hitherto published results for bulk samples of $(BiFeO_3)_x$-$(BaTiO_3)_{1-x}$ solid solutions [2]. The magnetoelectric properties of $0.6BiFeO_3$-$0.4BaTiO_3$ are even better. This sample exhibits the strongest magnetoelectric coupling of all the investigated samples – α_{ME} = 3.57 mV/A (Fig. 7b). Moreover, the frequency dependence of the α_{ME} coefficient is almost constant for all the samples above the threshold of 2 kHz, which makes these materials, especially $0.6BiFeO_3$-$0.4BaTiO_3$, potentially applicable in new magnetoelectric devices, e.g. magnetic field sensors.

Conclusions

The magnetic and magnetoelectric measurements conducted as part of this study showed that the investigated $(BiFeO_3)_x$-$(BaTiO_3)_{1-x}$ solid solutions possess both ferroelectric and weak ferromagnetic properties, depending on the composition of the sample and the sintering time and temperature. As x decreased from 0.9 to 0.7 the magnetic hyperfine field decreased as well. Moreover, the gradual structural transformation from rhombohedral to regular symmetry accompanies these changes, which was observed in X-ray diffraction patterns and confirmed by the Rietveld analysis. Significantly, different properties, i.e. the presence of the tetragonal phase and relatively higher values of the magnetic hyperfine field, are exhibited by samples where x = 0.6 and 0.5 due to their inhomogeneity. These samples, however, possess the best magnetoelectric properties in terms of their application.

References

1. Duong, G. V., Groessinger, R., Schoenhart, M., & Bueno-Basques, D. (2007). The lock-in technique for studying magnetoelectric effect. *J. Magn. Magn. Mater*., *316*, 390–393. DOI: 10.1016/j.jmmm.2007.03.185.
2. Yang, S. -Ch., Kumar, A., Petkov, V., & Priya, S. (2013). Room-temperature magnetoelectric coupling in single-phase $BaTiO_3$-$BiFeO_3$ system. *J. Appl. Phys*., *113*, 144101-1-5. DOI: 10.1063/1.4799591.
3. Kowal, K., Jartych, E., Guzdek, P., Lisińska-Czekaj, A., & Czekaj, D. (2015). Magnetoelectric effect in $(BiFeO_3)_x$-$(BaTiO_3)_{1-x}$ solid solutions. *Mater. Sci.-Poland*, *33*(1), 107–112. DOI: 10.1515/msp-2015-0012.
4. Kowal, K., Kowalczyk, M., Czekaj, D., Jartych, E., Lisińska-Czekaj, A., & Czekaj, D. (2015). Structure and some magnetic properties of $(BiFeO_3)_x$-$(BaTiO_3)_{1-x}$ solid solutions prepared by solid-state sintering. *Nukleonika*, *60*(1), 81–85. DOI: 10.1515/nuka-2015-0018.
5. Wodecka-Duś, B., & Czekaj, D. (2011). Synthesis of $0.7BiFeO_3$–$0.3BaTiO_3$ ceramics: thermal, structural and AC impedance studies. *Arch. Metall. Mater.*, *56*(4), 1127–1136. DOI: 10.2478/v10172-011-0126-5.
6. Park, T., Papaefthymiou, G. C., Viescas, A. J., Lee, Y., Zhou, H., & Wong, S. S. (2010). Composition-dependent magnetic properties of $BiFeO_3$-$BaTiO_3$ solid solution nanostructures. *Phys. Rev. B*, *82*(2), 024431-1–10. DOI: 10.1103/PhysRevB.82.024431.
7. Kumar, M. M., Shankar, S., Thakur, O. P., & Ghosh, A. K. (2015). Studies on magnetoelectric coupling and magnetic properties of (1-x)$BiFeO_3$-x$BaTiO_3$ solid solutions. *J. Mater. Sci.-Mater. Electron.*, *26*(3), 1427–1434. DOI: 10.1007/s10854-014-2557-z.
8. Gotardo, R. A. M., Viana, D. S. F., Olzon-Dionysio, M., Souza, S. D., Garcia, D., Eiras, J. A., Alves, M. F. S., & Cotica, L. F. (2012). Ferroic states and phase coexistence in $BiFeO_3$-$BaTiO_3$ solid solutions. *J. Appl. Phys*., *112*(10), 104112-1–7. DOI: 10.1063/1.4766450.
9. Chandarak, S., Unruan, M., Sareein, T., Ngamjarurojana, A., Maensiri, S., Laoratanakul, P., Ananta, S., & Yimnirun, R. (2009). Fabrication and characterization of (1-x)$BiFeO_3$-x$BaTiO_3$ ceramics prepared by a solid state reaction method. *J. Magn.*, *14*(3), 120–123. DOI: 10.4283/JMAG.2009.14.3.120.
10. Ismailzade, I. H., Ismailov, R. M., Alekberov, A. I., & Salaev, F. M. (1981). Investigation of the magnetoelectric (ME)H effect in solid solutions of the systems $BiFeO_3$-$BaTiO_3$ and $BiFeO_3$-$PbTiO_3$. *Phys. Status Solidi A-Appl. Mat.*, *68*, K81–K85. DOI: 10.1002/pssa.2210680160.
11. Kiyanagi, R., Yamazaki, T., Sakamoto, Y., Kimura, H., Noda, Y., Ohyama, K., Torii, S., Yonemura, M., Zhang, J., & Kamiyama, T. (2012). Structural and magnetic phase determination of (1-x)$BiFeO_3$-x$BaTiO_3$ solid solution. *J. Phys. Soc. Jpn.*, *81*(2), 024603. DOI: 10.1143/JPSJ.81.024603.
12. Kumar, M. M., Srinivas, A., & Suryanarayana, S. V. (2000). Structure property relations in $BiFeO_3$/$BaTiO_3$ solid solutions. *J. Appl. Phys.*, *87*(2), 855–862. DOI: 10.1063/1.371953.
13. Wang, T. H., Ding, Y., Tu, C. S., Yao, Y. D., Wu, K. T., Lin, T. C., Yu, H. H., Ku, C. S., & Lee, H. Y. (2011). Structure, magnetic, and dielectric properties of (1-x) $BiFeO_3$-x$BaTiO_3$ ceramics. *J. Appl. Phys.*, *109*(7), 07D907. DOI: 10.1063/1.3554253.
14. Kim, J. S., Cheon, C. I., Lee, C. H., & Jang, P. W. (2004). Weak ferromagnetism in the ferroelectric $BiFeO_3$–$ReFeO_3$–$BaTiO_3$ solid solutions (Re=Dy,La). *J. Appl. Phys*., *96*, 468–474. DOI: 10.1063/1.1755430.
15. Jartych, E., Pikula, T., Kowal, K., Dzik, J., Guzdek, P., & Czekaj, D. (2016). Magnetoelectric effect in ceramics based on bismuth ferrite. *Nanoscale Res. Lett.*, *11*, 234(8pp.). DOI: 10.1186/s11671-016-1436-3.
16. Kostiner, E., & Shoemaker, G. L. (1971). Mössbauer effect study of $Bi_2Fe_4O_9$. *J. Solid State Chem.*, *3*(2), 186–189. DOI: 10.1016/0022-4596(71)90025-9.